Melt Viscosity of Acrylic Copolymers

TOHRU NAGAI, YUICHI KIMIZUKA, ETSUKO NAKAMURA, and JUN'ETSU SETO, *Sony Corporation Research Center, 174 Fujitsukacho, Hodogaya-ku, Yokohama, 240 Japan*

Synopsis

The melt flow behavior of methyl methacrylate (MMA) copolymerized with methyl acrylate (MA) was measured and analyzed in terms of the molecular structure of the copolymers. Measurement was done by using a capillary rheometer in the shear rate range from 6×10^0 to 3×10^3 s^{-1} and in temperatures from 160°C to 280°C. The Newtonian flow pattern appeared in lower shear rate and higher temperature regions. However, with increasing shear rate at lower temperature, viscosity decreased to a constant slope on a logarithmic scale. The melt fracture arose at the critical shearing stress point S_c of 6×10^6 dyn/cm^2. A die swell also appeared in the shear rate range larger than 1×10^6 dyn/cm^2, and its maximum value was two times larger than that of the capillary diameter. The decrease in viscosity with increasing shear rate is explained in terms of the apparent energy of activation in flow E_a^*. E_a^* also decreases with increasing shear rate. The exponential relation of E_a^* to η is maintained in the higher shear rate. The lowering of viscosity in lower shear rate, however, is attributed to not only the change in E_a^* but also the change in the volume of flow unit. The melt viscosity increases in inverse proportion to the MA content in the copolymers which form more flexible chains. Syndiotactic form of MMA has increased viscosity, caused by the rigidifying of segmented chains, rather than the strengthening of intermolecular interaction.

INTRODUCTION

Acrylic resins, e.g., methyl methacrylate (MMA), are known to have excellent transparency, good weatherability, and high thermal stability. Because of this, they are often poured into a mold to make various kinds of lenses and prisms, which require precise processability. The acrylic resins for these applications must flow more freely than those used to form sheets, which are subsequently molded to the desired form by applying a vacuum. Acrylic resins to be poured into a mold are given good fluidity by lowering their molecular weight or copolymerizing with other acrylic esters and so on. In most cases, the methyl acrylate MA is copolymerized with MMA.

In order to develop an acrylic resin with good moldability, it is important to investigate the flow property of MMA copolymers in the melt state in terms of molecular structure and composition.

McCrum et al.[1] have reported that the glass transition temperature T_g lowers as the ratio of MA increases, and Gall and McCrum[2] have reported those in MMA; stereoregularity is another factor with influences T_g.

Among the few papers which have reported the melt flow behavior of MMA which relates closely to processing, Lehmann[3] has reported that melt viscosity η increases in proportion to the minus Sth power of the exponential, where S denotes shearing stress, and Christmann and Knappe[4] have reported that, in PMMA with different molecular weight but approximately the same molecular weight distribution, the rheological equation between

Journal of Applied Polymer Science, Vol. 29, 3479–3490 (1984)
 CCC 0021-8995/84/113479-12$04.00

melt viscosity η and shear rate D can be described by a single invariant curve. And, though the structural parameters of the copolymer, such as the copolymer ratio and stereoregularity, are thought to affect viscosity in the melt state, we could find even fewer papers which discussed this point.

In this paper the flow behavior of the MMA–MA copolymer, that is, the flow pattern, die swell, melt fracture, and apparent energy of activation, was investigated. The relationship between the molecular structure and melt viscosity is then discussed.

EXPERIMENTAL

Materials

The acrylic resins used are listed in Table I. These resins were purchased from Mitsubishi Rayon Co., Ltd. and Asahi Chemical Industry Co., Ltd.

The molecular weight was measured by GPC (gel permeation chromatography) with THF as the diluent.

Melt Viscosity

A capillary rheometer manufactured by Iwamoto Seiki Co., Ltd. was used to obtain the melt viscosity. By measuring the extruder speed V (cm/s) and the extruder pressure P (dyn/cm^2), and putting them into the following equations, the melt viscosity η was calculated:

$$\eta = S/D \tag{1}$$

$$S = PR/\pi R_1^2/2L \tag{2}$$

$$D = 4Q/\pi R^3 \tag{3}$$

$$Q = \pi R_1^2 V \tag{4}$$

In the above equations, S is the shearing stress, D is the shear rate, R and R_1 are the radii of the capillary and the radius of the cylinder of reservoir,

TABLE I
Samples of Acrylic Copolymers

No.	$\overline{M}_w$ ($\times 10^4$)	$\overline{M}_w/\overline{M}_n$	T_g (°C)	f_{MMA}	ϕ_{syn}
1	8.7	1.9	92	0.81	0.86
2	6.8	1.9	93	0.82	0.90
3	7.0	1.8	98	0.85	0.91
4	7.5	2.0	100	0.87	0.78
5	7.5	1.9	110	0.93	1.00
6	10.2	1.9	115	0.96	1.00
7	7.3	1.7	114	0.98	1.00
8	6.6	1.9	100	0.83	0.66
9	7.0	1.8	99	0.82	0.67
10	7.2	1.8	101	0.83	0.78
11	6.8	1.9	104	0.84	0.84
12	6.8	1.9	105	0.84	1.00

respectively, L is the length of capillary, and Q is the flow rate of the extrudate.

Glass Transition Temperature

Glass transition temperature T_g was measured by TBA using an automated torsional braid analyzer manufactured by Toray Industries Inc. The heating rate was 1.25°C/min.

Determination of Molecular Structure

The molecular structure of the test samples was determined by their IR spectrum. An example of the IR spectra is shown in Figure 1. MMA ratio f_{MMA} was determined by the method[5] of Kotera et al. as follows. The methylene group (—CH_2—) has a characteristic absorption at 6.89 μm (point a in the figure), which appears in both MMA and acrylic acid esters. The methyl group (—CH_3) of MMA has an additional characteristic absorption at 6.73 μm (point b in the figure) which does not appear in acrylic acid esters. f_{MMA} is the ratio between these two absorption values.

Syndiotactic ratio ϕ_{syn} was determined by the method[6] of Baumann et al. Both syndiotactic and isotactic ratios have characteristic absorptions at 7.18 μm (point c in the figure) but only the syndiotactic ratio has a characteristic absorption at 9.41 μm (point d in the figure). ϕ_{syn} is the ratio between these two absorption values.

RESULTS AND DISCUSSION

Melt Viscosity

Figure 2 shows the typical relationship between melt viscosity and shear rate D of acrylic ester copolymers at various temperatures. The Newtonian flow region widens up to 10^2 s^{-1} of shear rate at higher temperatures, but, as the temperature decreases, the region shifts to a lower shear rate.

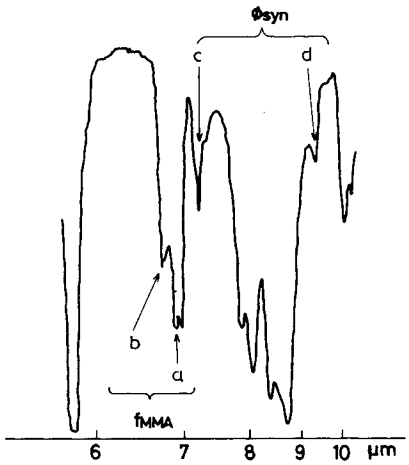

Fig. 1. IR spectrum of acrylic copolymer.

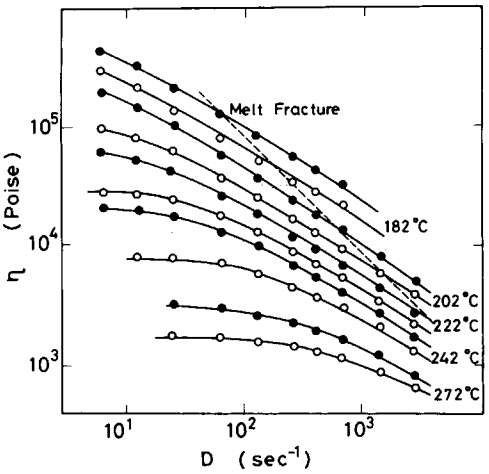

Fig. 2. Flow curve of acrylic copolymers: (●) sample no. 7; (○) sample no. 2.

In the non-Newtonian flow region, η decreases almost linearly to D and its slope, namely the flow index, is obtained as -0.63 at any temperature. Graessley[7] explained this behavior by assuming time constant τ_p to be required for the resin through the capillary and time constant τ_e to be required to recombine molecules which were deformed by shear force in flow. In the lower shear rate region, τ_p is larger than τ_e, so that melt viscosity is higher. The slope of the flow curve which decreases with increasing shear rate was calculated as -0.82 in monodisperse polymer and as -0.65 when molecular weight distribution $\overline{M}_w/\overline{M}_n$ equals 2. As can be seen in Table I, $\overline{M}_w/\overline{M}_n$ of our samples is nearly equal to 2, and the magnitude of the slope of the flow curve obtained is -0.63. This result agrees well with Graessley's result, offering further evidence that the mechanism of flow behavior can be explained in terms of intermolecular interactions.

The relationship between extruder pressure P and the ratios of capillary length to capillary diameters L/D is shown in Figure 3. A pressure drop of the entrance of the capillary was not observed, so it is clear that Bagley's correction[8] is not necessary for these copolymers.

Die Swell

It was observed that the diameter of the extruder passing through the capillary became larger, i.e., the die swell phenomenon, and also that in the higher shear rate region the shape of the extrudate exhibited reguler waves, i.e., the melt fracture phenomenon. These phenomena are shown in Figure 4. Figure 5 shows the relationship between swelling ratio d/d_0 and shearing stress S, where d and d_0 denote the diameter of the extrudate and capillary, respectively. d/d_0, which is nearly 1 when S is 10^6 dyn/cm^2, increases to about 2 when S is around 10^7 dyn/cm^2, irrespective of temperature. This suggests that the die swell is caused mainly by the normal stress difference.

The relationship between d/d_0 and S for two samples with different f_{MMA} is shown in Figure 6. d/d_0 values are nearly same for both samples when S is kept constant. From this result we can say that the normal stress difference is not affected by the value of f_{MMA}.

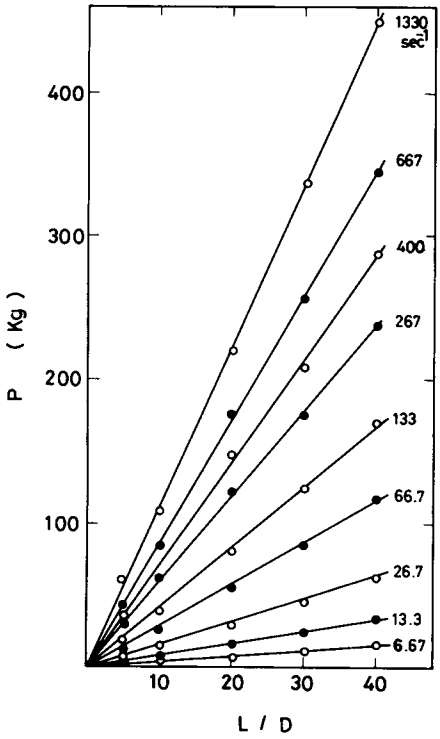

Fig. 3. Bagley's plot of sample no. 8.

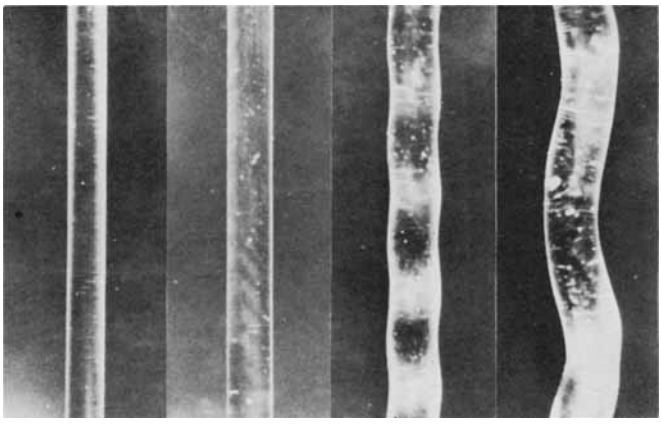

Fig. 4. Extrudates from capillary sample no. 8 at 178°C.

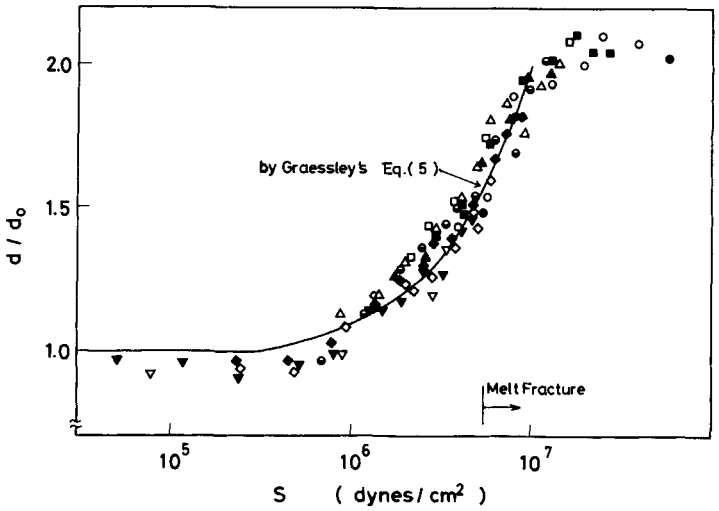

Fig. 5. Relationship between swelling ratio d/d_0 and shearing stress S: temperatures (°C): (●) 163; (○) 168; (■) 173; (□) 178; (▲) 188; (△) 198; (◐) 208; (◆) 218; (◇) 228; (▼) 243; (▽) 258.

Die swell is brought about by the recovery of the strain after passing through the capillary. Assuming a rubber elastic fluid whose compression energy is equal to recovery energy, Graessley et al.[9] derived following equation:

$$(d/d_0)^4 + 2(d/d_0)^{-2} - 3 = J_0^2 S^2/3 \tag{5}$$

$$J_0 = (2.2/1 + 2.1 \times 10^{-5} \overline{M}_w) J_R \tag{6}$$

$$J_R = \frac{2}{5} (\overline{M}_z \overline{M}_{z+1}/\overline{M}_w^2) \overline{M}_w/RT \tag{7}$$

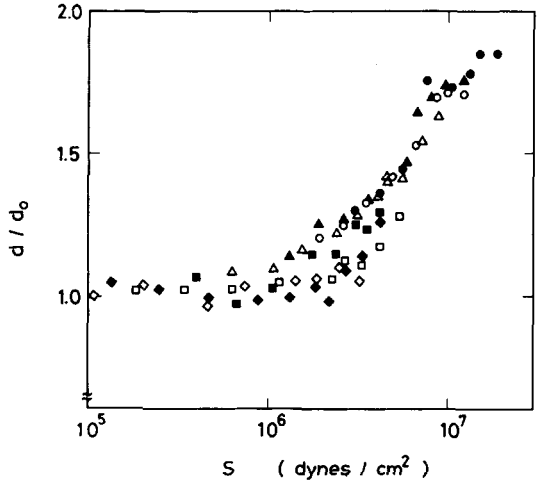

Fig. 6. Relationship between swelling ratio d/d_0 and shearing stress S in the two different f_{MMA} samples: (○,△,□,◇) no. 2; (●,▲,■,◆) no. 7; temperatures (°C): (○,●) 182; (△,▲) 202; (□,■) 222; (◇,◆) 242.

where J_0 and J_R are the true steady state shear compliance and the reduced steady state shear compliance, respectively, $\overline{M}_w$, $\overline{M}_z$, $\overline{M}_{z+1}$ is the weight-average, z-average, and (z + 1)-average molecular weight, respectively.

The solid line in Figure 5 was calculated from eq. (5) by substitution of 1.54 as d/d_0 and of 5×10^6 as S where measuring points gather in the vicinity. The curve agrees well with the plots of d/d_0 measured up to 10^7 dyn/cm^2 of shearing stress. The value of the true steady state shear compliance J_0, therefore, can be obtained from this curve as 6.4×10^{-7} cm^2/dyn. The value of J_0 calculated by applying eqs. (6) and (7) is 12.6×10^{-7} cm^2/dyn, where $\overline{M}_w = 6.6 \times 10^4$, $\overline{M}_z = 10.0 \times 10^4$, $\overline{M}_{z+1} = 13.5 \times 10^4$ were used. The value of J_0 as measured and calculated from Graessley's equation is so close that Graessley's model is applicable to our result. That is, the flow process is governed by the mechanism of deformation and recombination of intermolecular bondings in polymer chains.

Melt Fracture

As is shown in Figure 2, melt fractures were observed at the higher shear rate. A broken line was drawn through the critical stress points S_c, which initiated melt fracture on each curve in Figure 2. The result is a straight line with a slope of 45°. This indicates that S_c has a constant value of 6×10^6 dyn/cm^2, which is independent of temperature.

Bartoš[10] pointed out that the viscosity at the critical stress point S_c is closely related to the viscosity at Newtonian flow region η_N, i.e., the value of η_c/η_N is constant irrespective of temperature. The data of Figure 2 gives η_c/η_N as 6.3×10^{-2}, and, by using this value, η_N at the shear rate region, which cannot be measured by our apparatus, can be estimated, as is described in the following section.

Activation Energy

Log η is plotted against $1/T$ in Figure 7. Since a linear relation is obtained, apparent energy of activation E_a^* can be calculated by use of the slope.

The value of E_a^* is plotted against shear rate in Figure 8. The E_a^* decreases sharply in the lower shear rate region but more slowly in the higher shear rate region. The apparent energy of activation in Newtonian flow region E_0^* is calculated by use of the relationship $\eta_c/\eta_N = 6.3 \times 10^{-2}$ as 35 kcal/mol. This value almost equals the 34.0 kcal/mol obtained by Christmann and Knappe,[4] and the 35 and 39 kcal/mol obtained by Asami.[11] This suggests that the apparent energy of activation of acrylic acid ester copolymer is not so different from that of MMA homopolymers at the Newtonian region.

In sum, the activation energy in flow of acrylic acid ester copolymer measured by us decreases with increasing shear rate from 35 kcal/mol in the Newtonian flow region to 13 kcal/mol at shear rates higher than 10^3 s^{-1}.

According to Eyring's theory viscosity in melt state η can be expressed as:

$$\eta = h/v \cdot e^{-\Delta S^*/R} \cdot e^{E_a^*/RT} = Ze^{E_a^*/RT} \tag{8}$$

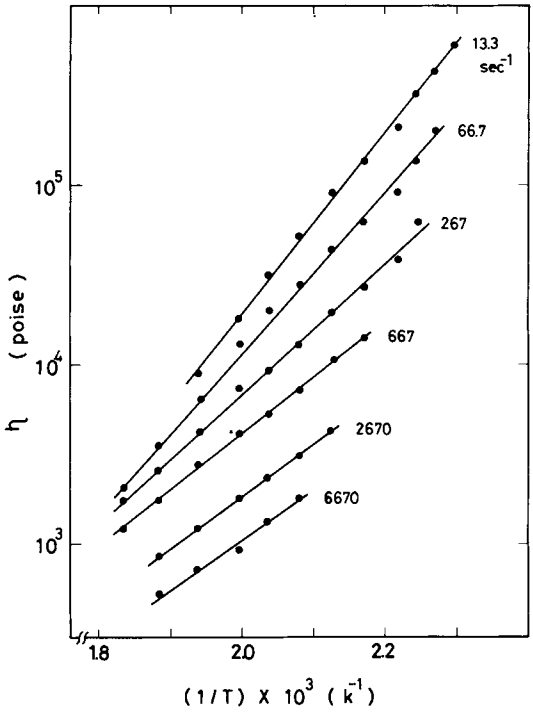

Fig. 7. Arrhenius plots of the melt viscosity of sample no. 8.

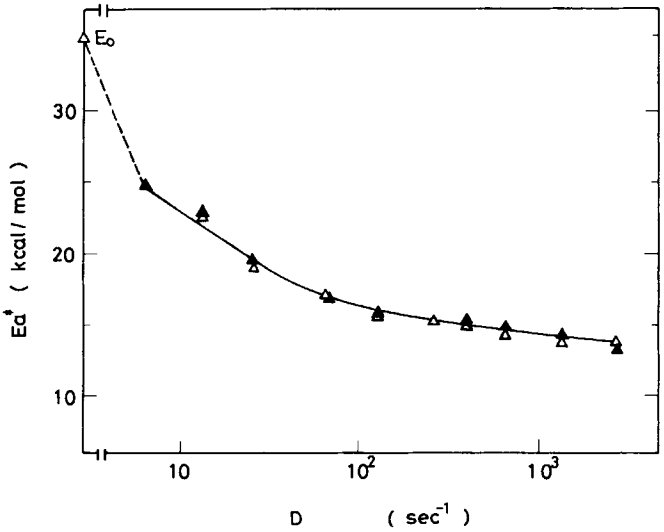

Fig. 8. Relation between apparent energy of activation E_a^* and shear rate D: (△) Sample no. 2 (f_{MMA} = 0.82); (▲) no. 7 (f_{MMA} = 0.98).

where h is Planck's constant, v is the volume of flow unit, and R is the gas constant. Viscosity η is given by apparent energy of activation E_a^*, activation entropy ΔS^*, and volume of flow unit v.

In linear polymer, the value of E_a^* caused by segmental flow is far less than that which might be expected from the magnitude of the molecular weight. Although from eq. (8) η is proportional to the E_a^*th power of the exponential, the relation measured deviates considerably from the theoretical slope shown by the solid line in Figure 9. That is, in the high shear rate region with low E_a^* the magnitude of the slope is nearly equal to the theoretical line, whereas in the low shear rate region with high E_a^* the deviation from the theoretical line becomes large. The decrease of η in the high shear rate region may be reasonably explained by the decrease of the potential barrier in the flow, but the decrease of the rate of viscosity in the low shear rate region cannot be explained only by the increase in the value of E_a^*. This can be attributed to the smaller value of the intercept of the E_a^* Arrhenius plot Z, as can be seen in Table II, and the larger volume of flow unit v, which is one of the factors constituting Z, in the low shear rate region. We consider that v decreases sharply as the shear rate increases. If the change in activation entropy ΔS^*, which is another factor constituting Z, contributes significantly to the value of Z, then ΔS^* must be larger in the low shear rate region. We recognize, of course, that this is inconsistent with the usual change of entropy.

As mentioned before, according to Graessley's model the intermolecular bonds of polymer chains keep deformed while passing through the capillary at a high shear rate. This mechanism corresponds to the decrease of E_a^* and the increase of the value of the intercept Z.

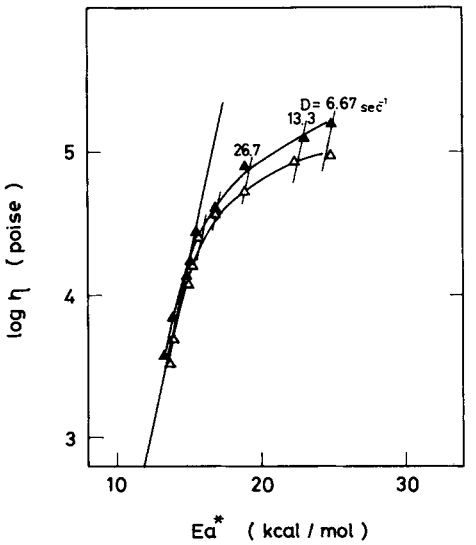

Fig. 9. Relationship between log η and E_a^*: (△) Sample no. 2 (f_{MMA} = 0.82); (▲) no. 7 (f_{MMA} = 0.98).

TABLE II
Intercept Z of Arrhenius Plot

Sample	No. 2	No. 7
f_{MMA}	0.82	0.98
ln Z at 66.7 s^{-1}	−8.86	−7.14
ln Z at 133 s^{-1}	−8.17	−6.73

Effect of Copolymerization

Figure 10 shows the relationship between the ratio of MMA of the copolymer, f_{MMA}, to the melt viscosity of η. η increases linearly with the increase of f_{MMA}.

Figure 10 also shows the behavior of the glass transition temperature T_g, which increases with the increase of f_{MMA}, similar to η. It is well known that, in the case of PMMA, α-CH_3 groups hinder the flexibility of the polymer chain and cause a higher T_g of 105°C. When MMA is copolymerized with a more flexible chain of MA whose T_g is 25.5°C, T_g lowers in proportion to the ratio of MA copolymerized. It is known that this lowering is associated with the dilution of the hindering effect of the α-methyl groups.

This hindering effect also appears in the flow behavior of the copolymer. That is, the rigidity of the polymer chains increases in proportion to the MMA ratio to MA, f_{MMA} so that the viscosity in the melt flow increases. A model of a segment of copolymer is shown schematically in Figure 11. The soft segment MA denoted by a white circle combines with the hard segment MMA denoted by a rod as in a flexible joint. When f_{MMA} increases and the composition of the copolymer approaches that of MMA homopolymer, then the segmental chain loses its flexibility and viscosity is increased.

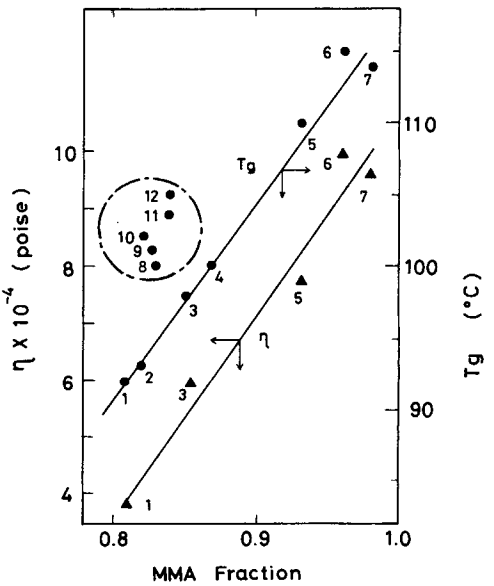

Fig. 10. Relation among f_{MMA}, η, and T_g (melt viscosity was measured at 188°C and $D = 10^2$ s^{-1}).

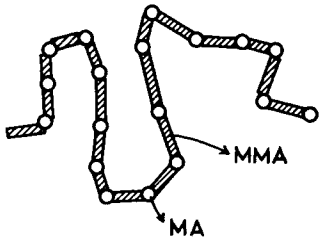

Fig. 11. Schematic representation of MMA–MA copolymer.

The relationship between log η and E_a^* in the two different copolymers with different f_{MMA} is shown in Figure 9. Sample no. 7 with larger f_{MMA} has a larger E_a^* value than that of sample no. 2 with smaller f_{MMA} at the same shear rate. The former sample also has a larger viscosity than the latter. We assume that the effect of f_{MMA} on viscosity can be explained by η's being proportional to ${}_eE_a^*/RT$.

Sample no. 2, which contains more flexible chains, deforms easily in flow and results in smaller E_a^*, and this leads to lower melt viscosity.

Effect of Stereoregularity

There exists stereoregularity in PMMA. In the syndiotactic form, a side chain appears alternately on both sides of the plane, including the main chain, but in the isotactic form a side chain appears on only one side of the chain. The glass transition temperatures of syndiotactic and isotactic PMMA were 105°C and 42°C, respectively. For some of our copolymers the T_g's cannot be expressed as a linear relation with f_{MMA}, and these T_g's are shown within a circle in Figure 10.

Figure 12 shows the effects of syndiotactic fraction ϕ_{syn} on T_g, and on η for these copolymers. The T_g is proportional to ϕ_{syn}, as is the same relation obtained by Gall and McCrum[2] for PMMA.

The viscosity η is also linearly related to the fraction of syndiotactic form, ϕ_{syn}, as is shown in the same figure. We consider this tendency to be caused by the decrease in flexibility of segmented chains.

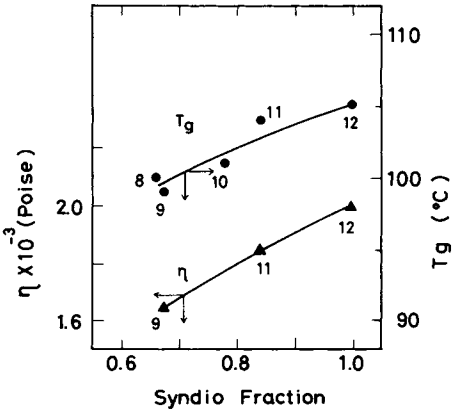

Fig. 12. Relation among syndiotactic fraction ϕ_{syn}, η, and T_g (melt viscosity was measured at 272°C and D = 2.7×10^1 s^{-1}).

We consider that this decrease in flexibility causes rigidifying of the segmented chains rather than strengthening of intermolecular interaction. In other words, when the syndiotactic fraction ϕ_{syn} increases, the rigidity of rod in the model in Figure 11 increases and causes an increase in η. This is also supported by the fact that the apparent energy of activation E_a^* slightly increases with increasing η.

CONCLUSIONS

The melt flow behavior of methyl methacrylate (MMA) copolymerized with methyl acrylate (MA) was measured and analyzed in terms of the molecular structure of the copolymers.

The viscosity decreased with increasing shear rate to be a flow index of -0.63. The melt fracture arose at the critical shearing stress S_c of 6×10^6 dyn/cm^2. A die swell appeared in the shearing stress region larger than 1×10^6 dyn/cm^2, and its maximum value was two times larger than that of the capillary diameter. These values were not changed by molecular weight, MMA–MA ratio, and stereoregularity of the acrylic copolymers.

The activation energy in flow E_a^* decreases with increasing shear rate. The exponential relation of E_a^* to η is maintained in the higher shear rate. The lowering of viscosity in lower shear rate, however, is attributed to not only the change in E_a^* but also the change in the volume of flow unit.

The melt viscosity increases in inverse proportion to the MA content in the copolymer which form more flexible chains. Syndiotactic form of MMA has increased viscosity, caused by the rigidifying of segmented chains, rather than the strengthening of intermolecular interaction.

References

1. N. G. McCrum, B. E. Read, and G. Williams, *Anelastic and Dielectric Effects in Polymeric Solids*, Wiley, New York, 1967, Chap. 8.
2. W. G. Gall and N. G. McCrum, *J. Polym. Sci.*, **50**, 489 (1961).
3. J. Lehmann, *Rheol. Acta*, **14**, 337 (1975).
4. L. Christmann and W. Knappe, *Colloid Polym. Sci.*, **252**, 705 (1974).
5. A. Kotera, M. Shima, K. Akiyama, M. Kume, and M. Miyazawa, *Bull. Chem. Soc. Jpn.*, **39**, 758 (1966).
6. U. Baumann, H. Schreiber, and K. Tessmar, *Makromol. Chem.*, **36**, 81 (1960).
7. W. W. Graessley, *J. Chem. Phys.*, **47**, 1942 (1967).
8. E. B. Bagley, *J. Appl. Phys.*, **28**, 624 (1957).
9. W. W. Graessley, S. D. Glasscock, and R. L. Crawley, *Trans. Soc. Rheol.*, **14**, 519 (1970).
10. O. Bartoš, *J. Appl. Phys.*, **35**, 2767 (1964).
11. K. Asami, *Acrylic Resins*, Nikkan Kogyo Shinbun, Tokyo, 1970, p. 82.

Received November 3, 1983
Accepted February 17, 1984